Elsevier Editorial System(tm) for Powder Technology
Manuscript Draft

Manuscript Number: POWTEC-D-14-01374R1

Title: CAPILLARY RHEOLOGY STUDIES OF INVAR 36 FEEDSTOCKS FOR POWDER INJECTION MOULDING

Article Type: Research Paper

Keywords: powder injection moulding; rheology models; INVAR 36; poly (ethylene glycol); cellulose acetate butyrate

Corresponding Author: Dr. Javier Hidalgo-García, Ph.D.

Corresponding Author's Institution: Carlos III University

First Author: Javier Hidalgo-García, Ph.D.

Order of Authors: Javier Hidalgo-García, Ph.D.; Antonia Jiménez-Morales, Ph.D.; Thierry Barriere, Prof.; Jean C Gelin, Prof.; José Manuel Torralba, Prof.

Abstract: Capillary rheology was used to determine shear viscosities of low expansion alloy INVAR 36 feedstocks for powder injection moulding (PIM) based on gas atomised powders and cellulose acetate butyrate (CAB) and poly ethylene glycol (PEG) binders. Different variables that describe the flow behaviour were analysed, in particular the relationships between viscosity of the melted feedstock with different conditions, such as shear rate ($\dot{\gamma}$), temperature (T), solid loading (Φ) and particle size (PS). The viscous behaviour was physically interpreted and discussed and a generalised rheological model that involves all of the dependant parameters: $\dot{\gamma}$, T, Φ and PS was proposed. The particular rheological behaviour of the feedstocks, which deviates from typical pseudoplastic behaviour, has a relevant correlation with the proposed model. Moreover, the model would be used when similar behaviours were observed in other systems.

*Cover Letter

Carlos III University of Madrid

Javier Hidalgo, PhD
Carlos III University of Madrid
Avda. Universidad 30, 28911, Leganés (SPAIN)

10 of December, 2014

Dear Editor-in-chief of Journal of Powder Technology:

I have sent original revised manuscript and figures by attached files of the manuscript "Capillary Rheology Studies of Invar 36 Feedstocks for Powder Injection Moulding" to Powder Technology. The authors confirm that the submitted manuscript is original and unpublished, is being submitted only to this editor and is not being considered for publication elsewhere. The authors confirm that all authors have participated in, read, and agree with the content and conclusions of the manuscript. The authors confirm that there is no conflict of interest regarding the financial supporter.

The present work has been carried out in the frame of an enterprises collaborative project granted by the Spanish Ministry of the Economy and Competitiveness and The European Funds for Regional Development (ECOPIM Ref. IPT-2011-0931-020000). The goal of the project is developing new potential binders for powder injection moulding PIM. In that respect, the micro metal injection moulding route of low coefficient of thermal expansion invar alloys was proposed and investigated for producing high property pieces. There are scarce works regarding powder injection moulding of invar alloys and to the best of the authors' knowledge there is none that uses these alloys combined with CAB based binders. Furthermore there are no works dealing with rheology studies of such combinations and rather few of CAB based feedstocks. We consider that the present is a very complete rheology study regarding these feedstocks. Almost all the aspects involving rheology were investigated, i.e the dependence of viscosity with temperature, shear rate, solid loading and particle size of the powders. The whole work aims to propose a single mathematical expression that takes into account all the viscosity dependant variables. We consider we are presenting a complete and relevant work that apart from the novelty of rheology studies of Invar 36 feedstocks could serve as a guideline for carry out PIM rheology of many other materials. We expect you consider all these works interesting to be published in your journal.

Some of the authors are research staff of the Carlos III University of Madrid (Spain) at the Materials Science and Engineering department and inside the powder technology group. The investigation group has expertise in very different types of powders including metal and ceramics. In the recent years, the main achievements focused on binder systems developing. The binder system used for Invar 36 powder is relatively novel and has demonstrate to be very suitable for micro PIM. The main author Dr. Javier Hidalgo-García has recently presented his thesis work in this topic under the supervision of the co-authoring Dr. Antonia Jimenez-Morales and Professor José Manuel Torralba as well as Prof. Thierry Barriere and Prof. Jean Calude Gelin. Prof. Thierry Barriere and Prof. Jean Calude Gelin belong to the Framche-Compté University (France) and to the Applied Mechanics and Microtechniques department of FEMTO-ST Institute of Besançon (France). They focused in process simulation combined with experimental work. All co-authors have extensive experience in powder technology and particularly in powder injection moulding field with more than 15 years of experience, with several PhD thesis work supervised and hundreds of publications and participation in international congresses.

I hope the reviewed manuscript is considered interesting in order to be published in this journal

Yours faithfully

Javier Hidalgo

Reviewer #1:

1. **English needs to be improved. The reviewed manuscript have been checked by Elsevier language polishing system.**

The manuscript was sent to Elsevier language polishing system and a copy of the invoice was enclosed in the reviewed version

2. In this paper, two different particle sizes were employed to evaluate the particle size influence. However, two types of powder size is not enough to evaluate the effects of particle size. At least three different particle sizes are demanded.

Regarding this comment, we agree with the reviewer that more particle sizes are needed. However, the supplier only offered us these two particles sizes for gas atomized Invar 36 powders. Moreover, as it is a not a material they commonly have in stock, we would to order a taylor-made powder and the delivery time could be out of a reasonable time. We have already tried with a D90 of around 50 microns water atomized powder from another supplier. The irregular shape introduced another shape factor to the equation. Moreover, with such a big powder we had lot of problems with flow instabilities during measurements in capillary rheometer. Therefore, these measurements were discarded for the present study. We expect these issues were considered. The fact that more particle sizes are needed is remarked in the text.

3. Page 5, line 4, authors mentioned the powder size as the d90 , The characteristic powder size is generally considered as d50. It should be changed.

This was changed, although d50 also appeared in the table describing particle size parameters

4. Authors divided viscosity curve into three stages. In Figure 3, there is no peculiarity to make a division for each stage. The viscosity curve seems a smooth curve. To satisfy the author's assumption as shown in Figure 3, related to microstructure, an additional evidence is required.

The assumption made to develop Figure 3 were based on literature review description of possible events occurring during the viscosity vs. shear rate curves and they were tried to be extrapolated to our material behaviour. The viscosity curve did not completely describe a pseudoplastic behaviour classically explained by a Cross model. There are some evidences on a the occurrence of a threshold value, but they also cannot be confirmed due to limitation of the capillary rheometer in the low shear rate range. Evidences on the assumptions would be difficult to obtain by other methods. The thin threads of feedstock coming out of the capillary were deformed due to gravity effect and stripped in the capillary exit. Therefore, although SEM inspection were tried, no concluding observations were made.

5. P. 7, line 4, authors mentioned that "the viscosity is dominated by hydrodynamic interaction……", The interaction among the powders is important for high powder volume fraction. More explanations about reason why particle-particle interaction can be neglected are demanded.

We are completely agree with this comment. Particle-particle interaction were not neglected, but obviously there was no mention of it in the text, sorry. It is true that for such high loading there is a

lot of particle-particle interactions but also the hydrodynamic effect of melt binder over particle motion. This paragraph was revised trying to clarify possible misunderstood with the term hydrodynamic and to include the particle-particle interactions.

6. P.7, A possible explanation regarding the correlation between shear rate effects and thermal analysis has nothing to do with shear rate effects. Thermal effects are not relevant to the main topic in this section regarding shear rate effect. Keep only the essential that are relevant in this section.

Thank you for this appreciation, this discussion was added demanded by a previous revision to discard the possibility of any other thermal effect like measuring viscosity close to the melting point of CAB. We decided to keep it like this if doubts still arises for any other reader.

7. Comment, if comparison analysis between models of hypothetical possible and experimental result which is an experimental result, for instance SEM image, is added to verify the author's model, paper will be more improved.

For us it would be of a great joy to come to this kind of verifications, but as was discussed in the point 4, by the way we did not manage to make a clear observation of the processes described

*Graphical Abstract (for review)

Invar 36

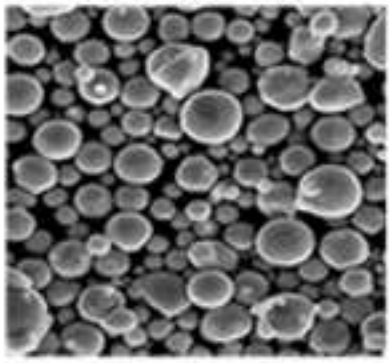

CAB

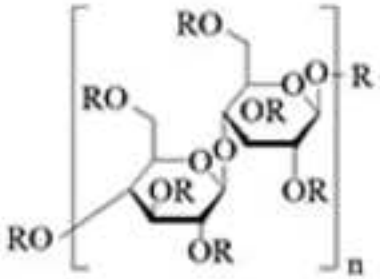

PEG

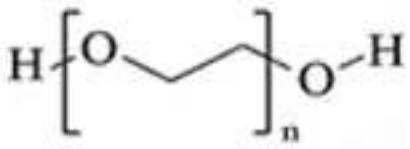

Feedstocks

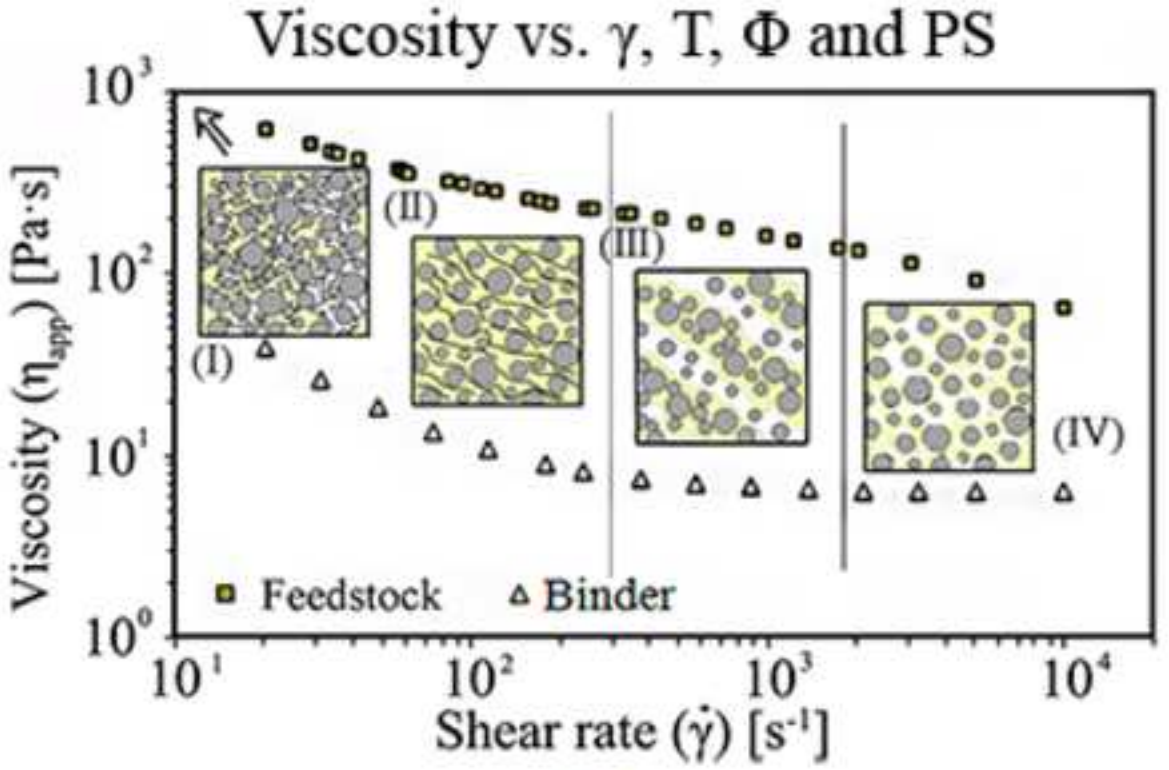

Viscosity model

Abstract

Capillary rheology was used to determine shear viscosities of low expansion alloy INVAR 36 feedstocks for powder injection moulding (PIM) based on gas atomised powders and cellulose acetate butyrate (CAB) and poly ethylene glycol (PEG) binders. Different variables that describe the flow behaviour were analysed, in particular the relationships between viscosity of the melted feedstock with different conditions, such as shear rate ($\dot{\gamma}$), temperature (T), solid loading (Φ) and particle size (PS). The viscous behaviour was physically interpreted and discussed and a generalised rheological model that involves all of the dependant parameters: $\dot{\gamma}$, T, Φ and PS was proposed. The particular rheological behaviour of the feedstocks, which deviates from typical pseudoplastic behaviour, has a relevant correlation with the proposed model. Moreover, the model would be used when similar behaviours were observed in other systems.

***Highlights (for review)**

Hihglights

- We studied the rheology of feedstocks based on Invar 36 and CAB and PEG binders
- We measured the viscosity at different conditions by capillary rheometer
- The behavior of the feedstocks was discussed and adjusted to viscosity models
- We propose a model that describes the viscous behavior of the studied feedstocks

CAPILLARY RHEOLOGY STUDIES OF INVAR 36 FEEDSTOCKS FOR POWDER INJECTION MOULDING

J. Hidalgo[a*], *A. Jiménez-Morales*[a], *T. Barriere*[b], *JC. Gelin*[b] *JM. Torralba*[a,c]

a Materials Science Department at Carlos III University of Madrid, Avd. Universidad 30, 28911, Leganés (Spain) jhidalgo@ing.uc3m.es, toni@ing.uc3m.es

b Applied Mechanics Department at FEMTO-ST Institute, 26 Rue de l'Epitaphe, 25000, Besançon (France) thierry.barriere@univ-fcomte.fr, jean-claude.gelin@univ-fcomte.fr

c IMDEA Materials Institute, Eric Kandel 2, 28906, Getafe (Spain) josemanuel.torralba@imdea.org

* Corresponding author: Avd. Universidad 30, 28911, Leganés (Spain), telephone: +34916249963, e-mail: jhidalgo@ing.uc3m.es

Abstract

Capillary rheology was used to determine the shear viscosities of low expansion alloy INVAR 36 feedstocks for powder injection moulding (PIM) based on gas atomized powders and cellulose acetate butyrate (CAB) and poly-ethylene glycol (PEG) binders. Different variables that describe the flow behaviour were analysed, in particular, the relationships between viscosity of the melted feedstock with different conditions, such as shear rate ($\dot{\gamma}$), temperature (T), solid loading (Φ) and particle size (PS). The viscous behaviour was physically interpreted and discussed, and a generalized rheological model was proposed that involves all of the dependant parameters: $\dot{\gamma}$, T, Φ and PS. The particular rheological behaviour of the feedstocks, which deviates from typical pseudoplastic behaviour, has a relevant correlation with the proposed model. Moreover, the model can be used when similar behaviours are observed in other systems.

Keywords: powder injection moulding**,** rheology models, INVAR 36, poly-(ethylene glycol), cellulose acetate butyrate.

1. Introduction

Powder injection moulding (PIM) is a manufacturing process that is suitable for the large-scale production of net shape complex geometries and reduced-size pieces of a large variety of materials processed as fine powders. In many cases, PIM remains the only viable method for the production of a particular part or product.

The PIM process involves the use of a mixture of polymer type components with metallic or ceramic powders that are injected into a mould cavity at temperatures above the softening point of the polymer part. It has been extensively demonstrated that the knowledge of the rheology of feedstocks at different conditions is a key issue to allow for the proper optimization of process settings, to obtain good quality parts and thus to optimize production costs [1-5].

The viscous behaviour of a fluid depends on multiple variables. Feedstocks in their fluid melted states are complex compared with single phase fluids. The feedstocks are composed of a multiple component binder, which remains in a melted state during feedstock fabrication and the injection moulding stage, and a high charge of fine particulate solid powders. Hausnerova [6] compiled a thorough review about feedstock rheology and indicated that the interpretation of rheological experimental data for PIM feedstocks is not always a simple task.

In this work, capillary rheology is used to determine the shear viscosity of Invar 36 alloy feedstocks based on atomized powders and cellulose acetate butyrate (CAB) and poly-ethylene glycol (PEG) binders. Invar 36 is a low expansion alloy with a high dimensional stability at temperatures below 230 ºC. The rheology of these feedstocks has scarcely been investigated. Conventionally, different analytical models are used to describe the melted feedstock's flow behaviour and viscosity dependence on different processing conditions, such as the shear rate ($\dot{\gamma}$), temperature (T), solid loading (Φ) and particle size (PS).These models commonly relate viscosity with one or a maximum of two of these variables. In this work, a global viscosity model involving all of the dependent variables, including $\dot{\gamma}$, T, Φ and PS, was proposed and discussed for describing the viscous behaviour of the studied feedstocks. This global viscosity model allows for the evaluation of the viability of feedstocks for their use in the development of PIM components and the development of improved computational algorithms.

2 Theoretical remarks

The viscosity of a feedstock depends on the viscosity of the binder and how it is influenced by the presence of powder particles and temperature. Some good reviews with examples of viscosity models

and their applicability to PIM feedstocks can be found in Lapointe [7] and Honek [8]. All of these models relate one or two viscosity dependant variables in a single expression.

The model proposed by Cross [9] has been extensively demonstrated to adequately describe the influence of the shear rate on the viscosity of a binder in a wide range of shear rates. Eq. 1 is based on the Cross model but considers the occurrence of a yield shear stress (τ_y) that must be overcome to allow the binder to begin to flow. The existence of a yield shear stress is controversial but well accepted in the PIM field.

$$\boldsymbol{\eta(\dot{\gamma}) = \tau_y \cdot \dot{\gamma}^{-1} + \frac{\eta_0}{1+(k\cdot\dot{\gamma})^n}} \qquad (1)$$

The η_0 coefficient represents the asymptotic value of the viscosity for low shear rates in the Cross model when the fluid behaviour is Newtonian, before the shear thinning region takes over. In the modified model, Eq. 1, η_0 does not represent the shear viscosity at a zero shear rate due to τ_y. The n coefficient, sometimes referred as the flow index, is related with the shear thinning behaviour at the pseudoplastic region of the curve. The k coefficient depends on the material and is related to the shear rate region in which the flow changes from Newtonian to pseudoplastic, i.e., when the shear thinning begins. These parameters, hence, have an influence on the viscosity curve shape.

At temperatures sufficiently far above the feedstock softening point, the relationship between the viscosity and the temperature commonly follows an Arrhenius-type relationship, as expressed in Eq. 2:

$$\eta(T) = B \cdot \exp\left(\frac{E_a}{R\cdot T}\right) \qquad (2)$$

where T is the absolute temperature, B refers to a reference viscosity value, R is the gas constant and E_a represents the flow activation energy. The activation energy is a measurement of the dependence of the viscosity on temperature. This dependence is important in PIM because high activation energies, which imply a high dependence of the viscosity on temperature, can cause rapid changes in viscosity during mould filling, which may lead to defects in the resulting parts.

A large number of works are found in the literature regarding the study of the relationship between viscosity and the solid loading. All of the models relate the relative viscosity (η_{rel}), which is the value

of the feedstock viscosity divided by the binder viscosity, to the solid loading content (Φ). These models fulfil the condition of an infinite value for the relative viscosity when solid loading is at the critical value Φ_{crit}**.** The Mills model [10] (Eq. 3) is one possible model to describe the relationships between viscosity and solid loading. A and m are dimensionless coefficients.

$$\frac{\eta(\phi)}{\eta_{BINDER}} = A \cdot \left(\frac{\phi_{crit}}{\phi_{crit}-\phi}\right)^{m} \qquad (3)$$

In addition, Contreras [11] demonstrated that the particle size and the particle size distribution are influential factors on the rheology of PIM feedstocks. Senapati [12] obtained a correlation coefficient, $10 \cdot C_u/d_{50}$, that relates the particle size characteristics to the viscosity of high filled ash slurries. The coefficient of uniformity, C_u, is defined as the ratio d_{60}/d_{10}. C_u has been demonstrated to be a useful parameter to relate the particle size distribution with the powder packing capacity and thus with the properties of the final piece. The higher the value of C_u, the larger the range of the particle sizes in the sample and hence the larger the effect on the viscosity of the feedstocks with high solid loading concentrations.

Larsen et al. [13] proposed the so-called equivalent viscosity model for PIM feedstocks that combined temperature, solid loading, shear rate and particle size distribution variables in one single expression. This model fitted well with the experimental results, considering the particular viscous behaviour of the feedstocks studied.

Based on the equivalent viscosity model, but considering the results with our Invar 36 feedstocks, the following expression (Eq. 4) is proposed in this work:

$$\eta(\dot{\gamma}, T, \phi, PS) = \frac{C_u}{d_{50}} \cdot \exp\left(\frac{E_a}{R \cdot T}\right) \cdot \left(\frac{\tau_y}{\dot{\gamma}} + \left(\frac{\eta_0}{(1+k \cdot \dot{\gamma}^{n})}\right)\right) \cdot \left(\frac{\phi_{crit}}{\phi_{crit}-\phi}\right)^{m} \qquad (4)$$

To develop Eq. 4, the Cross modified, Arrhenius and Mills models, along with particle size dependence, were first evaluated and demonstrated to be suitable single variable models or relations to describe the viscous behaviour of the studied feedstocks. Next, the global viscosity model (Eq. 4) was proposed and experimentally validated.

3. Experimental procedure

Figure 1 Particle size distribution curves for INV1 and INV2.

Two different particle sizes of gas atomized INVAR 36 alloy powders were used in this study to evaluate the particle size influence on viscosity. The morphology of the powers is spherical, typical of powders that are atomized in gas. The INVAR 36 alloy consists of 36 wt% of Ni and Fe balanced with other trace elements. The powders were supplied by Sandvik Osprey Ltd. (UK). The coarsest powder, with a d_{50} of 7.7 μm, is referred to as INV1, and the finest, with a d_{50} of 3.8 μm, is referred to as INV2. The particle size distribution curves for INV1 and INV2 are plotted in Figure 1, and the main particle size parameters are collected in Table 1. The S_w parameter, which represents the width of the particle size distribution [14], is similar in both powders. Hence, the effect of the particle size distribution width on the rheology of the feedstock was assumed to not affect the results. Both powders have a spherical morphology, as seen in the scanning electron microscopy (SEM) images presented in Figure 2.

Table 1 Particle size distribution parameters.

Each powder was mixed with a binder system based on a combination of compounds of several molecular weights, employing poly-(ethylene glycol) (PEG) (supplied by Sigma-Aldrich) and two types of cellulose acetate butyrates (CAB) (supplied by Estman) with a variable content of acetyl, butyryl and hydroxyl groups. This type of binder was selected due to its ecological features because PEG is able to be eliminated by water and CAB comes from a cellulosic natural raw source. The binder component content and component specifications are included in Table 2.

Figure 2 SEM images of the different powders: a) INV1 and b) INV2.

Several feedstocks with a variable content of solid loadings ranging from 57.5 to 67.5 vol.% were prepared in a HaakeRheomex twin sigma rotor internal mixer; the mixing parameters were constant for all of the feedstocks. These samples allowed for the evaluation of solid loading influence on the viscosity of the feedstocks. The feedstocks were mixed at a temperature of 150 ºC and a rotor speed of 50 rpm for one hour to ensure the homogenization of all of the components.

Table 2 Binder composition.

For capillary rheology measurements, a Rosand RH2000 double piston capillary rheometer with a capillary of 1 mm in diameter and 30 mm in length (L/D ratio 30) was used. The pressure drop values at the capillary entrance were acquired for different shear rates and temperature conditions by a pressure transducer with a maximum pressure registration of 70 MPa. Those values were then converted into shear viscosity values. The apparent shear rate range studied covers shear rates from 20 to 10000 s^{-1}. Three temperatures were evaluated: 150 ºC, 160 ºC and 170 ºC; in addition, for the INV2 67.5 vol.%, 180 ºC was also evaluated. To ensure the reproducibility of the data acquisition, the tests were replicated five times for each condition, and an average value is presented.

The non-linear regression of the experimental data was performed by solving a minimization problem of the RSS_p parameter (Eq. 5) using algorithms based on the generalized reduced gradient method GRG [15], where η_{mes} is the measured viscosity, and η_{est} is the estimated value of the viscosity, according to variable values of the model parameters being optimized.

$$\mathbf{RSS_P} = \sum_{\mathbf{i=1}}^{\mathbf{m}} \frac{(\boldsymbol{\eta}_{\mathbf{mes}} - \boldsymbol{\eta}_{\mathbf{est}})^{\mathbf{2}}}{\boldsymbol{\eta}_{\mathbf{mes}}} \qquad (5)$$

4. Results and discussion

4.1 Viscosity dependence on the shear rate

Figure 3 shows the flow behaviour of the binder at 160 ºC and a INV2 feedstock at 160 ºC and 60 vol.%. To some extent, this behaviour was reproduced in the other feedstocks at different solid loadings and temperatures (see also Figure 7).

Figure 3 Binder and INV2 feedstock viscosity dependence with the shear rate and models of hypothetical possible situations at the different regions of the feedstock's curve. Each model visually attempts to show the feedstock's features at three different curve stages. The curves correspond to experiments performed at 160 ºC and the solid loading of 60 vol.%.

Focusing on the feedstocks, three stages are typically observed in their viscosity vs. shear rate curves. These curves may be explained as follows:

(i) At low shear rates, a pseudoplastic behaviour is observed both for the binder and the feedstock. It seems that viscosity would be very high at values near 0 s^{-1} according to the observed trend, which suggests the possibility of the occurrence of a threshold shear stress that must be surpassed for the

feedstock to begin to flow. Some authors relate the observation of a yield stress with the occurrence of this particle network structure within the melt [6, 16]. Hence, in this very low shear rate region, a network structure was assumed (see schematic explanation in Figure 3(I)) with a rigid structure formation due to the presence of a high number of particles and interactions between the binder and the powder particles. These particles are likely homogeneously distributed within the binder matrix, but the presence of certain heterogeneities in the particle distribution or the formation of agglomerates cannot be dismissed.

(ii) This theorized network structure, which is relatively stable at very low shear rates, is destroyed as the shear rate increases. Thus, the viscosity is dominated by hydrodynamic interactions between the binder and the powder particles and, for high solid loading feedstock, by particle-particle interactions as the bulk begins to flow. This results in shear thinning as particles and polymer orientate and order (Figure 3(II)) in the flow direction to allow inter-particle motion, as discussed by Husband [17]. Then, the shear thinning rate of the feedstock reduces in the intermediate shear rate region (approximately 200-300 s^{-1}). A possible explanation of this behaviour, specially observed at low temperatures, would be that CAB is playing the role of a particle filler instead of a binder because it is not melted or softened. In previous works, a thermal analysis of these feedstocks was performed by differential scanning calorimetry (DSC) [18]. Pure CAB551 and CAB381 exhibited a glass transition temperature (softening temperature) at 125.5 ºC and 147.7 ºC, respectively. A melting point at higher temperatures was not observed. However, this glass transition was not observed in the experiments with the binder and the feedstock, and most likely, these temperatures were lowered due to the mixture with PEG and powders. Therefore, the theory of CAB acting as a particle filler is not conclusive. Another possible explanation of this behaviour may be the segregation of the binder phases. In this case, the effect of high shear stresses separates the PEG from CAB. The most viscous phase (in this case CAB) then contains a higher portion of particles because they would be more effectively retained when a high shear is applied. These are the bases of slip band theory that, in the case of binders systems containing PEG, is well explained and argued by Chuankrerkkul [19]. Hence, low particle content PEG regions will be formed (Figure 3(III)). The flow is favoured at these low viscosity regions, but, in contrast, is

reduced in the CAB high particle and high viscosity regions, reducing the shear thinning effectiveness with shear rate.

(iii) Until the end of this intermediate region, it could be said that the rheological behaviour of the feedstock is, to some extent, dominated by the binder behaviour. Thereafter, other factors begin to dominate. Instabilities in the viscosity measurements begin to be observed. A possible explanation of a more pseudoplastic-like behaviour at high shear rates would be the rupture of the slip bands that are hypothetically formed. Some authors relate a shear thinning behaviour to the breakage of agglomerates, as reported by Hausnerova [6]. This breakage of agglomerates could also be a plausible explanation of the shear thinning because the viscosity can be reduced by disruption of CAB highly particles concentration regions (see Figure 3(IV)).

This behaviour was well described by a Cross modified model (Eq. 1). In Table 3, the fitting coefficients of Eq. 1 are shown for different values of viscosity variables: temperature, solid loading and particle size. Most of these coefficients greatly varied with the experimental set of conditions, with no clear dependence on the variables that are modified. Hence, this model is limited to describe the viscous behaviour of the studied feedstocks and requires specific measurements at each set of conditions.

The feedstock in this work did not exhibit typical pseudoplastic behaviour in the shear rate range occurring during injection commonly desired in MIM. If segregations actually occurred, then they could create flaws than might worsen the final part properties. Nevertheless, the shear thinning behaviour and the low viscosity measured (below the recommended maximum of 10^3 Pa·seg at typical shear rates occurring during injection) will allow for a proper mould cavity filling. Despite the fact that these feedstocks did not exhibit typical pseudoplastic behaviour, they were tested to produce Invar 36 micro parts that, after the entire MIM process, apparently did not exhibit flaws and exhibited mechanical properties consistent with those expected for this material [20, 21]. Therefore, it was concluded that these feedstocks have a potential use for a variety of different applications.

Table 3 Resulting coefficients after a non-linear regression experimental data adjustment to a Cross modified model of different measuring conditions.

4.2 Relative viscosity dependence on solid loading

The relative viscosity was taken at a constant shear rate. Several authors indicated that if the relative viscosity is obtained at a constant shear rate, non-Newtonian suspensions of small particles (non-fibrous) do not approach an asymptotic plateau at high shear rates, as in the case of relative viscosity defined at the same shear stress [22, 23]. Regardless of the fact that many theoretical equations have been primarily set up for relative viscosities at the same shear rate, the shear stress should be taken as independent for non-Newtonian suspensions. However, according to Hausnerova et al.[24], the values of relative viscosity were obtained at a constant shear rate to avoid difficulties involved in extrapolations in the complex patterns of the flow curves.

Figure 4 shows the relative viscosity vs. solid loading experimental data for INV1 and INV2 feedstocks and the adjustment curves to a Mills model (Eq. 3). At low solid loading, there was almost no variation of the relative viscosity, but from a certain solid loading, this tendency varied and then the relative viscosity grew abruptly. The critical solid loading can be shorted out, considering the asymptotic trend to infinite viscosity at solid loadings near this critical value. The different values obtained for INV1 and INV2 are explained by its different sizes and packing capacities. The critical solid loading, as well as the exponent m, varies slightly with the temperature and the shear rate chosen (see Table 4). From the results, it can be concluded that there is a good fitting of the Mills model to the experimental data.

Table 4 Examples of Mills model coefficients resulting from the fitting of experimental data curves at different temperatures and shear rates.

Figure 4 Relative viscosity vs. solid loading for INV1 and INV2 feedstocks at 160 ºC and 1000 s^{-1}. The straight and dashed curves represent the adjustment of the experimental data to the Mills model.

4.3 Temperature dependence

Figure 5 Example of the linearization viscosity dependence on temperature for INV2 60 vol.%.

The activation energy can be easily deduced from the linearization of (Eq. 2) by taking the natural logarithm of both sides of the expression if the final experimental points follow this relationship. The

slope of the resulting straight line representing ln (η) versus the inverse of temperature corresponds to E_a. Figure 5 shows an example of ln (η) versus 1/T plot for INV2 60 vol.% and presents the corresponding lines obtained by the linear regression of the data points. Some representative values of the assessed E_a for different conditions of the shear rate and solid loading are included in Table 5.

Table 5 Values of the activation energies for INV1 and INV2 at several conditions.

The multiple correlation coefficients, R^2, reveal a suitable adjustment of the experimental data to the Arrhenius relation in most of the cases. The activation energy varies depending on the shear rate, the solid loading content and the particle size.

4.4 Particle size dependence

Studying the ratio of the INV2/INV1 viscosities, a relatively constant average factor of 1.69±0.3 was obtained for 160ºC to 170ºC and 65 vol.% conditions, which is very close to the 1.929 value obtained for the ratio of the $D_{60}/D_{10}\cdot D_{50}$ values of both powders. However, for 60 vol.% and for other solid loadings under lower temperature conditions, this result is only valid for the high shear rates region, as can be observed in Figure 6. This result could be explained by considering that at low shear rates, as discussed previously, the binder dominates the feedstock viscous behaviour. This dominance is more evident as the solid loading decreases, and thus, the binder content increases. However, this result is also evidence that at high shear rates and high solid loadings, the powder particles exert the primary influence on the viscous behaviour. In addition to the results observed, more particle sizes should be evaluated in the future to properly validate the model. Water atomized powders with a d_{50} of approximately 30 µm (but with a d90 greater than 50 µm) were also mixed with the binder used in this work, and the resulting rheology was investigated. Although these large powders exceeded the standards for MIM, with a recommended particle size no larger than d90 < 20 µm, they were still investigated. The irregular shape that characterized these water atomized powder particles introduced another shape factor to the equation. Moreover, larger powder particles led to flow instabilities during measurements in capillary rheometer; as a result, no reproducible and reliable data were obtained. Therefore, these measurements were discarded for the present study.

Figure 6 Comparison between INV2 and INV1 feedstock viscosities for 60 vol.% and 65 vol.% and different temperatures. The relationship between the INV2 and INV1 particle size distributions is plotted as a straight line.

4.5 Generalised viscosity model

In the previous sections, the viscosity behaviour of the Invar36 feedstocks was evaluated and related to different viscosity models in terms of the relationship of viscosity with one single variable at a time. However, the coefficients of the mentioned models depended on other viscosity variables apart from the one being evaluated. This section will discuss the convenience of the use of a model that relates all of the studied viscosity variables with the viscosity in a single equation (Eq. 4).

Considering the critical solid loading established via the Mills model (Eq. 3), despite the variation of this coefficient with temperature and shear rate, a value of 71 vol.% and 68.5 vol.% can be considered for INV1 and INV2 powders, respectively. Moreover, for INV1 and INV2, the E_a coefficient can be considered relatively constant at the solid loading range from 60 vol.% to 65 vol.% and for the shear rate range above 500 1/s. In this interval, an average value of 42.3 $kJ \cdot mol^{-1} \cdot K^{-1}$ is estimated for both INV1 and INV2. Therefore, the coefficients τ_y, η_0, n, k and m were defined as variable coefficients, whereas Φ_{crit} and E_a were fixed at constant values during the model fitting to the experimental curves.

Some representative results of the model adjustment to the experimental date are presented in Table 6 and Figure 7 for INV1 and INV2. As can be observed, the predicted curves exhibit good correlation with the experimental points. Table 7 includes the average values obtained for η_0, m and n for INV2 and different solid loadings at the three studied temperatures.

Figure 7 Some examples of the curves fitting to the global viscosity model (dashed lines). Different viscosity variables, such as temperature, shear rate, solid loading and particle size, were varied: a) INV1 60 vol.&, b) INV2 60 vol.%, c) INV1 60 vol.% and d) INV2 65 vol.%.

Table 6 Resulting coefficients after curve fitting with the model described in Eq. 4 of the experimental points at different temperatures. Φ=65 vol.%, Φ_{crit}=68.6 vol.%, Ea=42.3 kJ/(mol·K).

The coefficients that were most compliant and sensible to other coefficients variation were η_0 and k. The influence of different variables on Eq. 4 coefficients is described below:

- Coefficient k has the most erratic and inconsistent behaviour. This erratic behaviour may be explained by the limited shear rate range at high sear rates, where the curve turns again into being more pseudoplastic. The k coefficient determines where the curve changes its tendency

from Newtonian to pseudoplastic. The limited number of points at this region may cause errors in determining this coefficient during model fitting.

- The predicted values of η_0 vary with the temperature and the powder content but remain quite similarly independent of these variables and powder type. The dependence of η_0 on temperature may be explained by a dominating influence of the binder on the feedstock viscosity. In fact, the values obtained for η_0 are equivalent to those obtained for the binder in the intermediate shear rate range; thus, this coefficient may be related to the binder viscosity. However, there is also a relationship of this coefficient with solid loading, as is reflected in Table 7.
- The coefficient m appears to be very stable with regard to temperature and particle size, but varies with solid loading. This coefficient does not influence the shape of the curve, but does influence the displacement along the viscosity axis.
- The coefficient n is another coefficient that appears to vary slightly with temperature and particle size; however, this behaviour only occurs at high solid loadings. The n coefficient determines the pseudo-plasticity, i.e., the shear thinning, of the feedstocks; on average, the pseudo-plasticity increases with solid loading.
- Regarding τ_y, this coefficient remains constant under all of the conditions evaluated, with a value of approximately 1060 Pa. This coefficient could be considered as a reference threshold value of the shear stress that must be exceeded if the feedstock flow is to occur. This coefficient influences the curve behaviour in the low shear rate region.

Table 7 Average values of η_o, m and n at different solid loading values for INV2

Although the proposed global viscosity model can be used in Invar 36 feedstocks to precisely describe its viscous behaviour at certain conditions, some of the expression coefficients have shown to be dependent on viscosity variables or influenced by other coefficients. There is no clear mathematical relationship between these coefficients and the viscosity variables or other coefficients. Nevertheless, the average values of the coefficients could be selected, and this expression may be used in computational algorithms to perform simulations of the injection process of the studied feedstocks.

5. Conclusions

The viscous behaviour of gas atomized Invar 36 alloy feedstocks based on CAB and PEG binders were thoroughly studied by varying several viscosity variables that influence the viscosity. Different models were adjusted to the experimental data obtained. Finally, a global viscosity model that combined these models was evaluated to describe the viscous behaviour of the Invar 36 feedstocks. It could be concluded that the proposed model is suitable to describe the viscous behaviour of CAB and PEG based feedstocks considering several variables at the same time. This type of model might also be suitable to predict the flow behaviour of other feedstocks if the appropriate coefficients are selected. These coefficients could be obtained via experimental data curve fitting by a non-linear regression. In the particular studied feedstocks, some of these coefficients exhibited a dependence on other equation variables. Nevertheless, an average value of the coefficient may be selected.

ACKNOWLEDGMENTS

The authors wish to acknowledge GUZMÁN GLOBAL S.L. and MIMTECH ALFA for their collaboration in the ECOPIM project (ref. IPT-2011-0931-20000) funded by the Spanish Ministry of the Economy and Competitiveness. Furthermore, the authors acknowledge the strong support from the ESTRUMAT projects (ref. S2009/MAT-1585) funded by the CAM-Consejería Educación Dir. Gral. Universidades e Investigación, and from the COMETAS project (ref. MAT2009/14448-C02-02), funded by the Spanish Ministry of the Economy and Competitiveness.

REFERENCES

[1] R. Zauner, C. Binet, D.F. Heaney, J. Piemme, Variability of feedstock viscosity and its correlation with dimensional variability of green powder injection moulded components, Powder Metallurgy, 47 (2004) 151-156.
[2] C. Zhiqiang, T. Barriere, L. Baosheng, J.C. Gelin, A vectorial algorithm with finite element method for prediction of powder segregation in metal injection molding, International Journal for Numerical Methods in Fluids, 70 (2012) 1290-1304.
[3] X. Kong, T. Barriere, J.C. Gelin, Determination of critical and optimal powder loadings for 316L fine stainless steel feedstocks for micro-powder injection molding, Journal of Materials Processing Technology, 212 (2012) 2173-2182.
[4] C. Zhiqiang, C. Quinard, K. Xiangji, T. Barriere, L. Baosheng, J.C. Gelin, Viscous Behaviours of Feedstocks for Micro MIM, Advanced Materials Research, 314-316 (2011) 713-718.
[5] Z.Q. Cheng, T. Barriere, B.S. Liu, J.C. Gelin, The Bi-phasic Numerical Simulation of Metal Co-injection Molding, International Journal of Material Forming, 1 (2008) 695-698.
[6] B. Hausnerova, Rheological characterization of powder injection molding compounds, Polimery, 55 (2010) 3-11.
[7] F. Lapointe, S. Turenne, B. Julien, Low viscosity feedstocks for powder injection moulding, Powder Metallurgy, 52 (2009) 338-344.

[8] T. Honek, B. Hausnerova, P. Saha, Relative viscosity models and their application to capillary flow data of highly filled hard-metal carbide powder compounds, Polymer Composites, 26 (2005) 29-36.
[9] M.M. Cross, Rheology of non-Newtonian fluids - A new flow equation for pseudoplastic systems, Journal of Colloid Science, 20 (1965) 417-&.
[10] P. Mills, Non-Newtonian behavior of flocculated suspensions, Journal De Physique Lettres, 46 (1985) L301-L309.
[11] J.M. Contreras, A. Jimenez-Morales, J.M. Torralba, Improvement of rheological properties of Inconel 718 MIM feedstock using tailored particle size distributions, Powder Metallurgy, 51 (2008) 103-106.
[12] P.K. Senapati, B.K. Mishra, A. Parida, Modeling of viscosity for power plant ash slurry at higher concentrations: Effect of solids volume fraction, particle size and hydrodynamic interactions, Powder Technology, 197 (2010) 1-8.
[13] G. Larsen, Z. Qiang Cheng, T. Barriere, B.S. Liu, J.C. Gelin, Simulation of micro injection moulding with emphasis on the formulation of feedstock viscosity: Use of non-equilibrium molecular dynamics for the determination of viscosity of multi-body fluid, 2011, pp. 714-719.
[14] D.F. Heaney, Powders for metal injection moulding, Handbook of metal injection

molding, Woodhead Publishing Limited, Cambirdge, 2012, pp. 50-63.
[15] L.S. Lasdon, S.K. Mitter, A.D. Waren, Conjugate gradient method for optimal control problems, Ieee Transactions on Automatic Control, AC12 (1967) 132-&.
[16] A.B. Metzner, Rheology of suspensions in polymeric liquids, Journal of Rheology, 29 (1985) 739-775.
[17] D.M. Husband, N. Aksel, W. Gleissle, The existence of static yield stresses in suspensions containing noncolloidal particles, Journal of Rheology, 37 (1993) 215-235.
[18] J. Hidalgo, J.P. Fernández-Blázquez, A. Jiménez-Morales, T. Barriere, J.C. Gelin, J.M. Torralba, Effect of the particle size and solids volume fraction on the thermal degradation behaviour of Invar 36 feedstocks, Polymer Degradation and Stability, 98 (2013) 2546-2555.
[19] N. Chuankrerkkul, P.F. Messer, H.A. Davies, Flow and void formation in powder injection moulding feedstocks made with PEG/PMMA binders Part 1 - Experimental observations, Powder Metallurgy, 51 (2008) 66-71.
[20] J. Hidalgo, A. Jiménez-Morales, T. Barriere, J.C. Gelin, J.M. Torralba, Water soluble Invar 36 feedstock development for μpIM, Journal of Materials Processing Technology, 214 (2014) 436-444.
[21] J. Hidalgo, A. Jiménez-Morales, J.C. Gelin, J.M. Torralba, Mechanical and functional properties of Invar alloy for μ-MIM, Powder Metallurgy, 57 (2014) 127-136.
[22] M.R. Kamal, A. Mutel, Rhelogical properties of suspensions in Newtonian and non-Newtonian fluids, Journal of Polymer Engineering, 5 (1985) 293-382.
[23] T. Kataoka, T. Kitano, M. Sasahara, K. Nishijima, Viscosity of particle filled polymer melts, Rheologica Acta, 17 (1978) 149-155.
[24] B. Hausnerová, P. Sáha, J. Kubát, Capillary Flow of Hard-Metal Carbide Powder Compounds, International Polymer Processing, 14 (1999) 254-260.

Figure1

Click here to download high resolution image

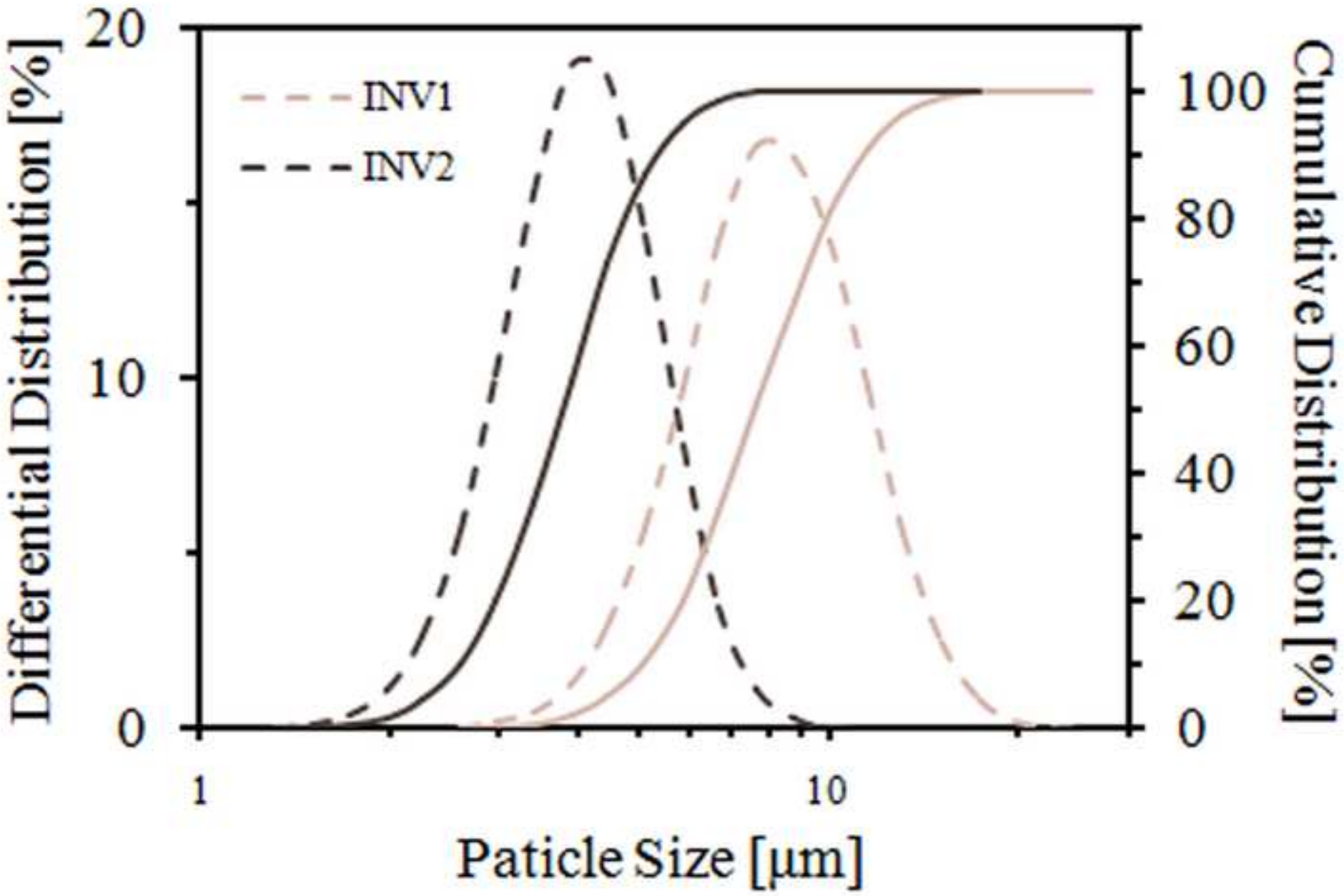

Figure2a

Click here to download high resolution image

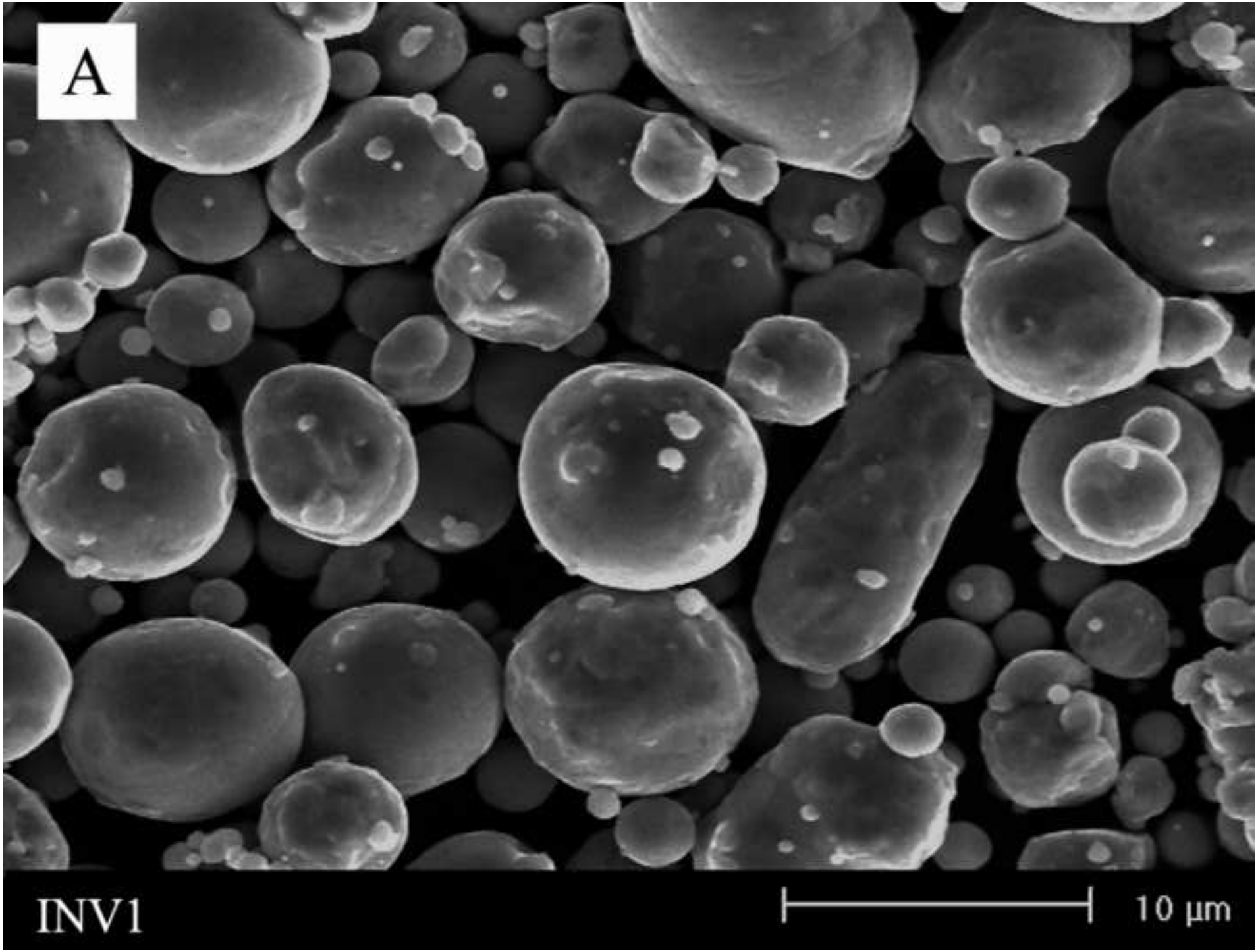

Figure2b

Click here to download high resolution image

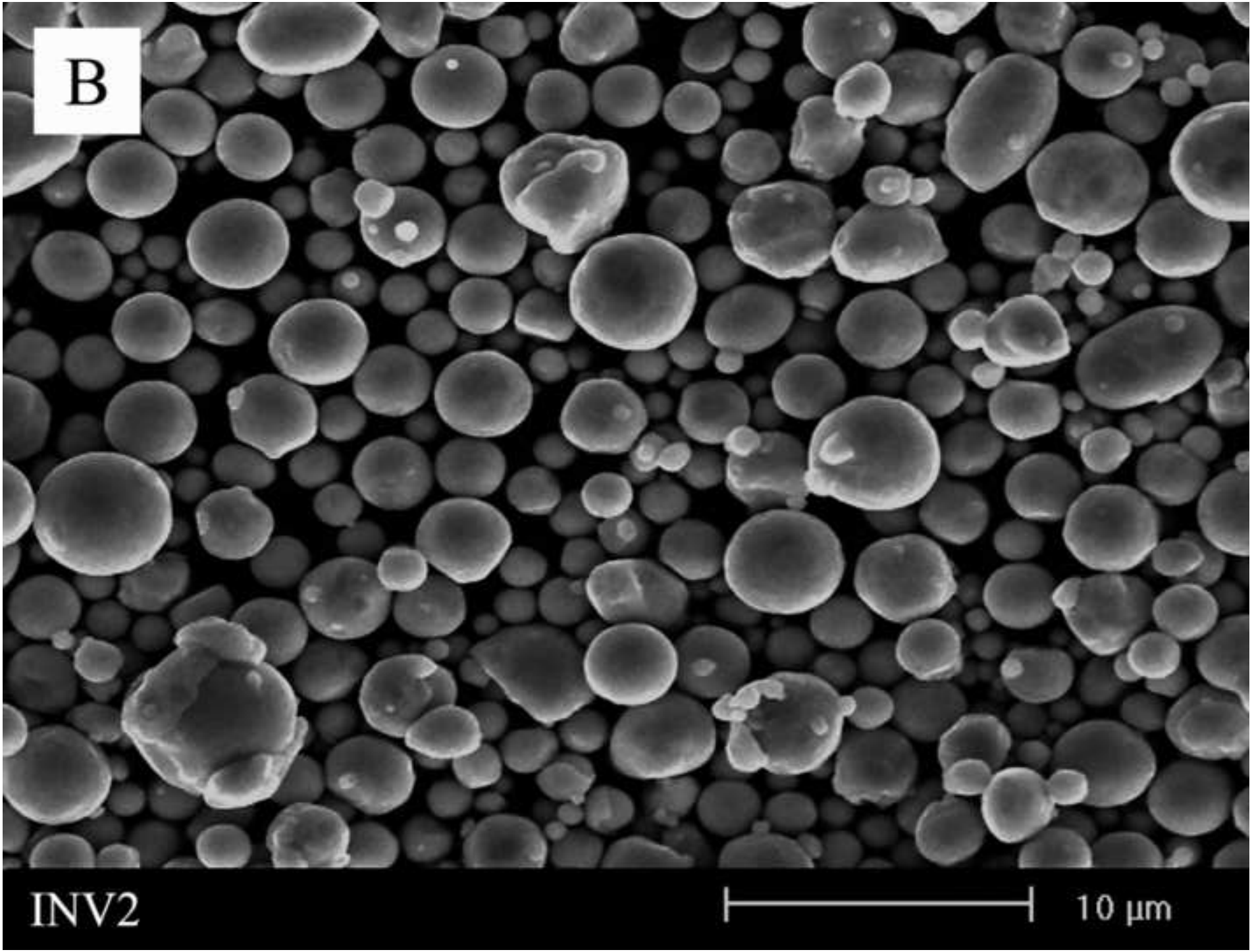

Figure3

Click here to download high resolution image

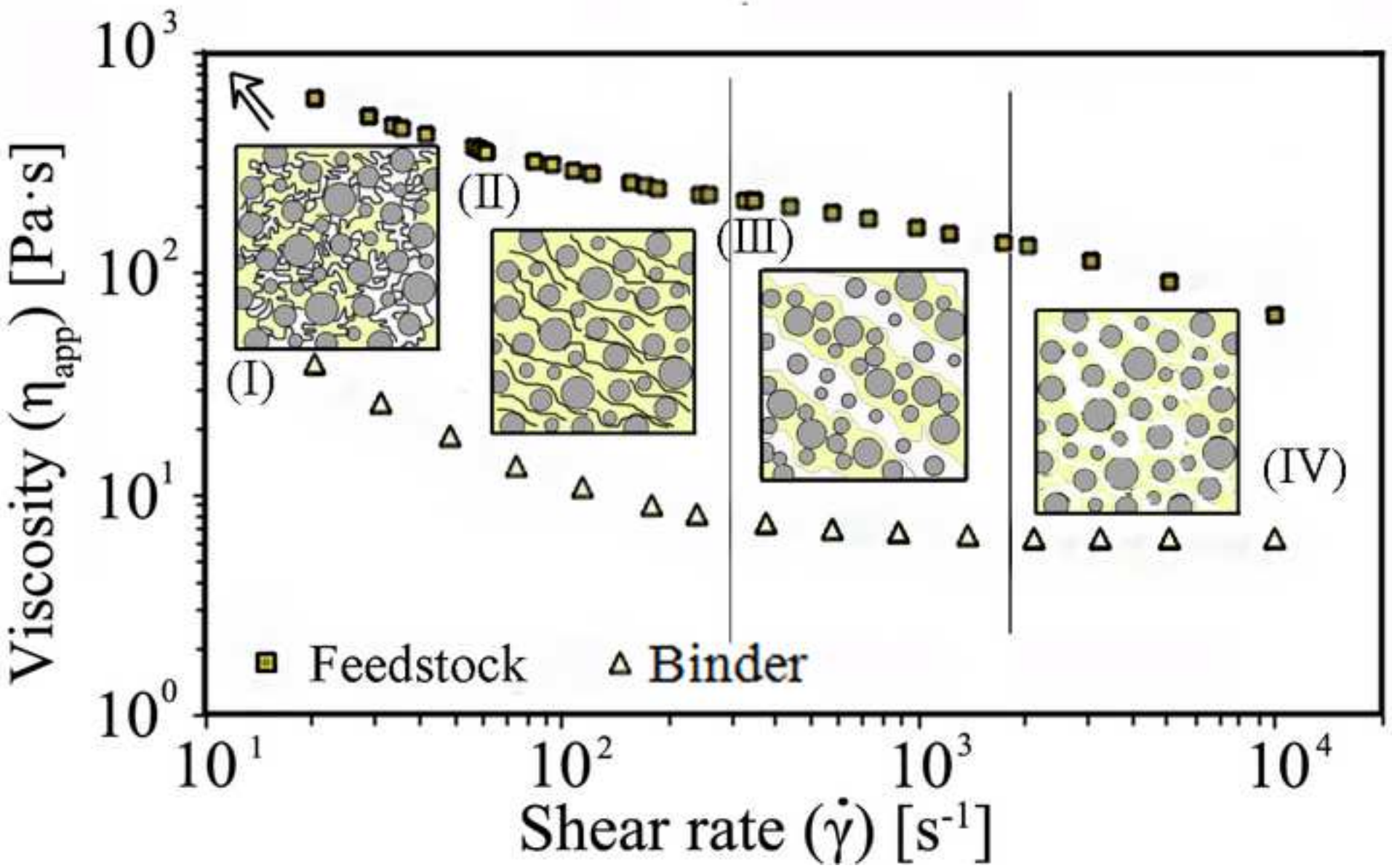

Figure4

Click here to download high resolution image

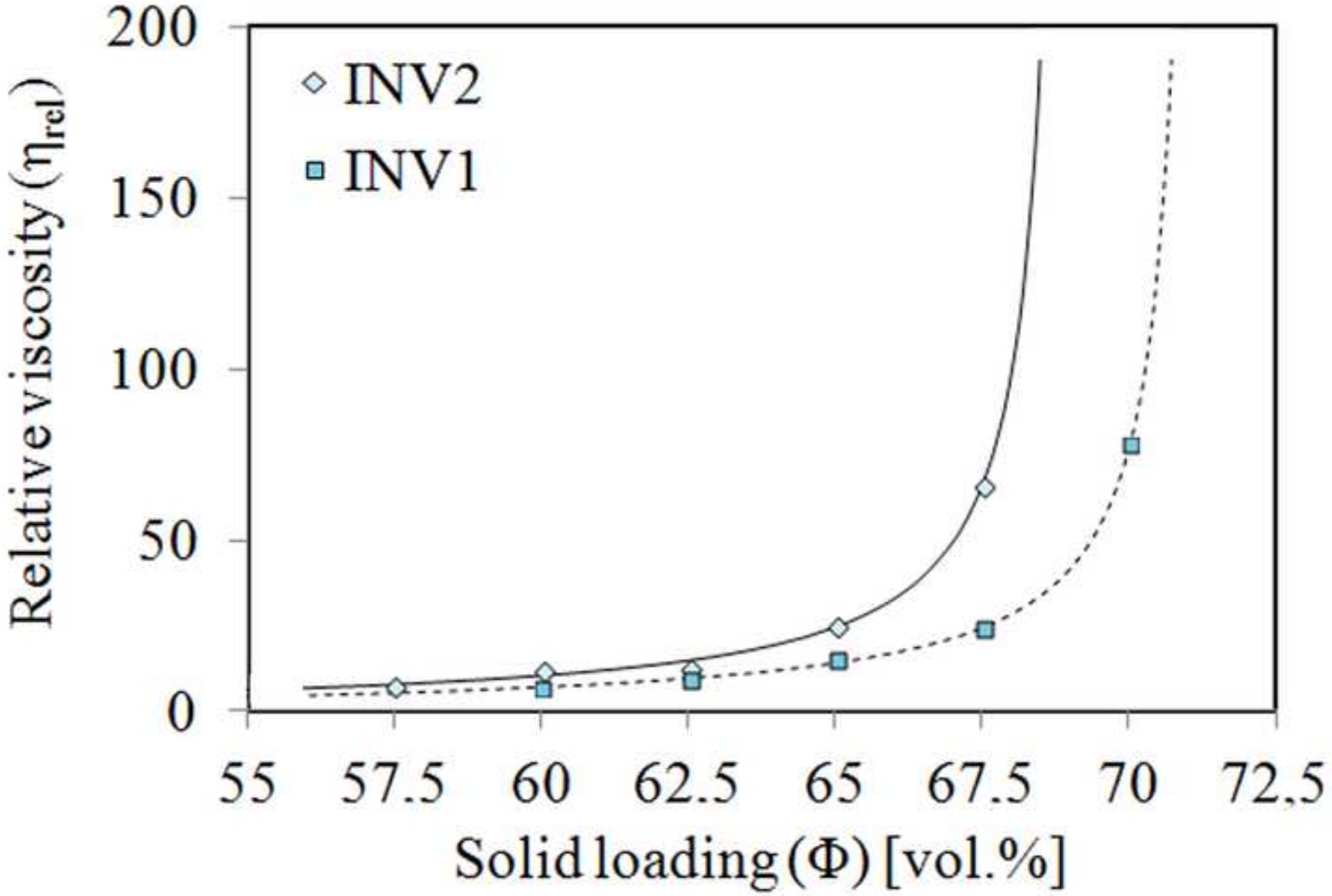

Figure5

Click here to download high resolution image

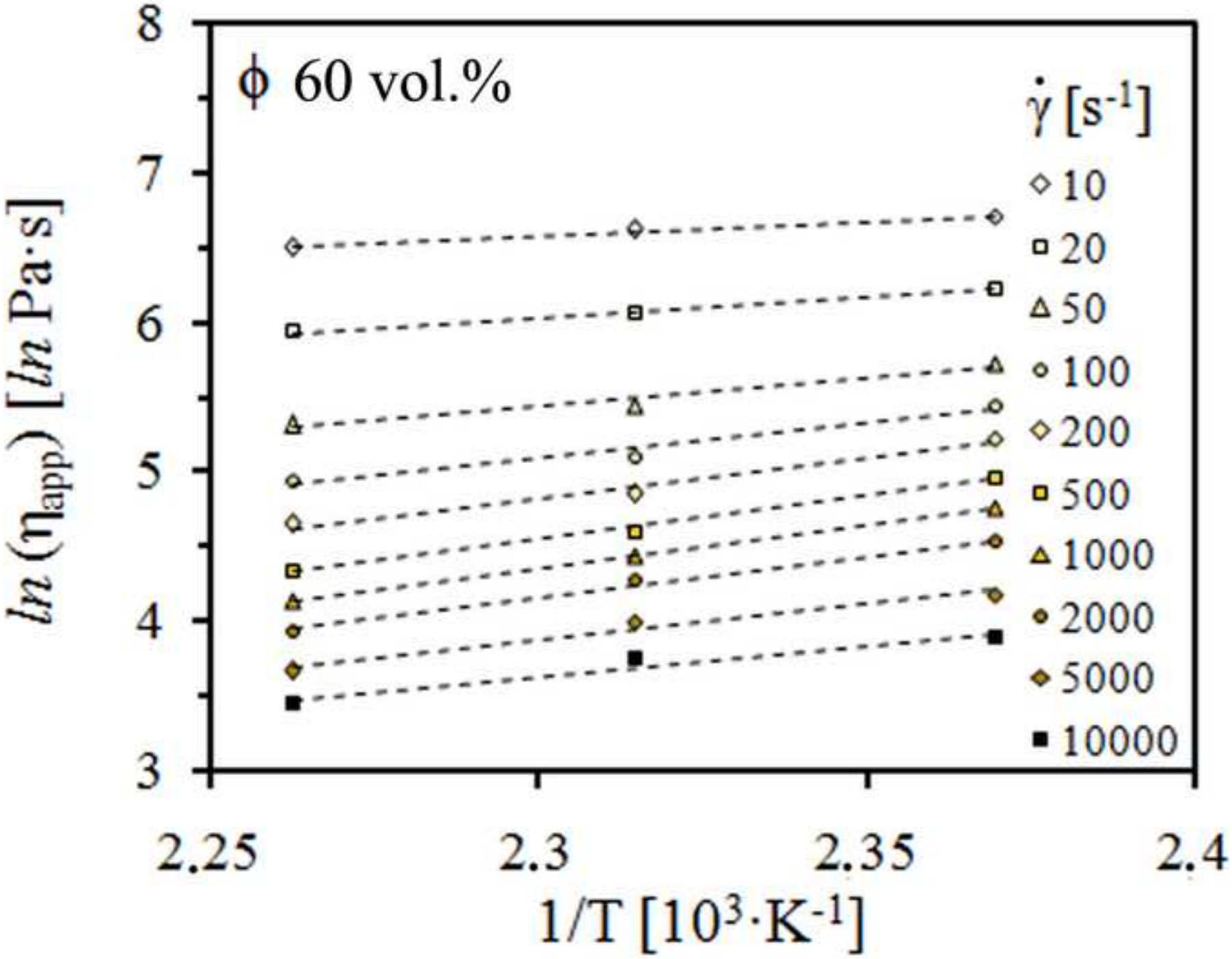

Figure6

Click here to download high resolution image

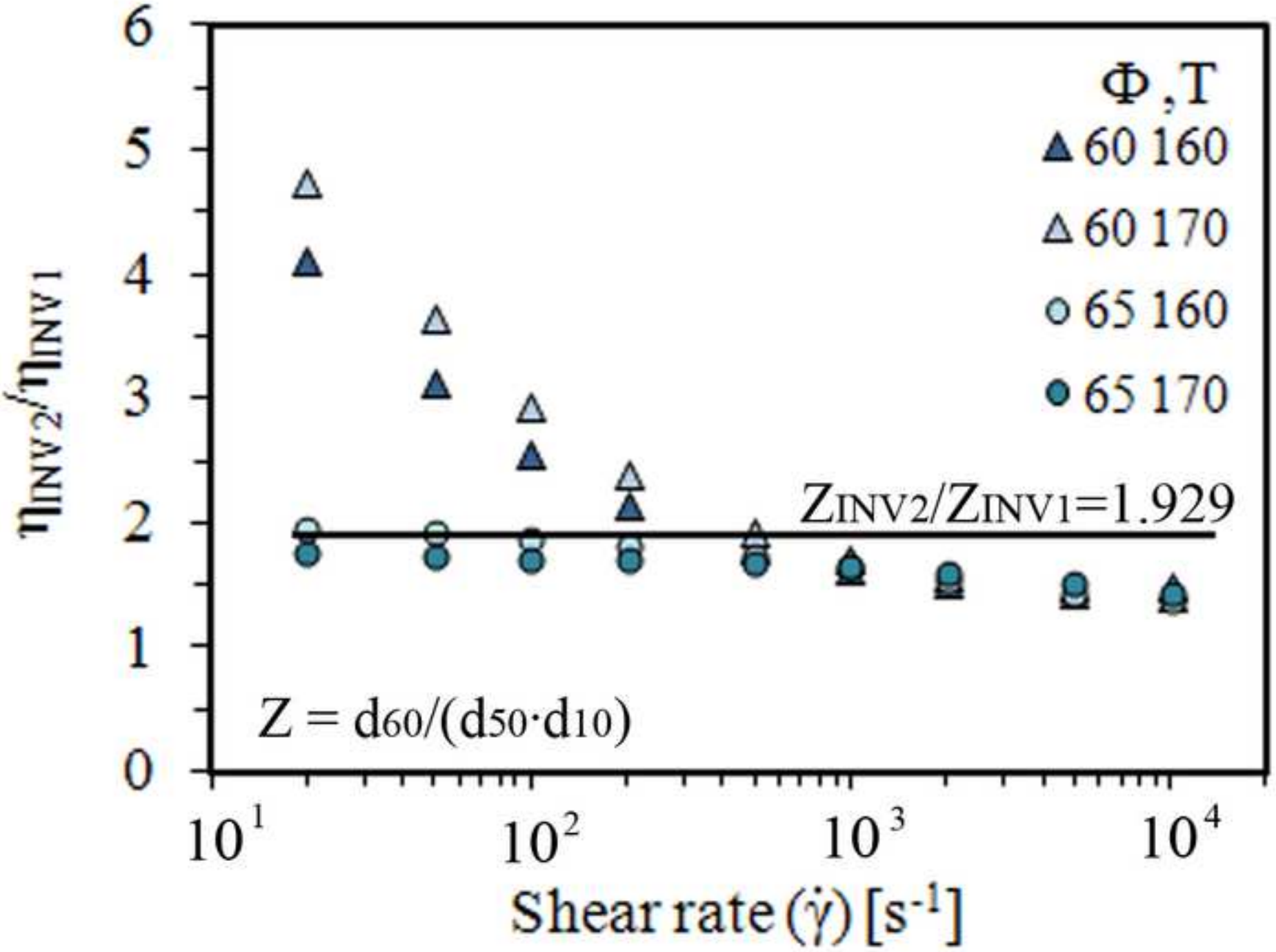

Figure7a

Click here to download high resolution image

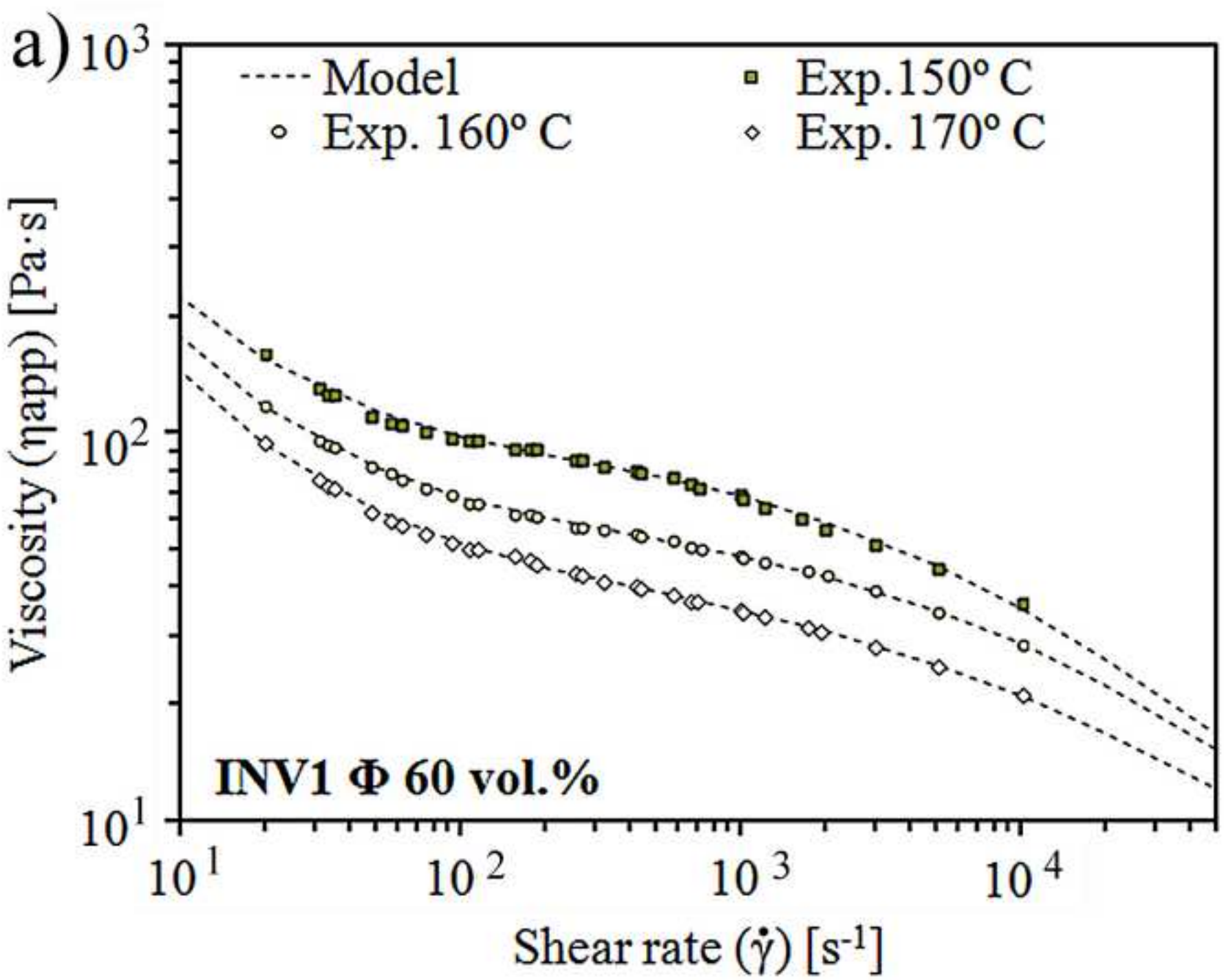

Figure7b

Click here to download high resolution image

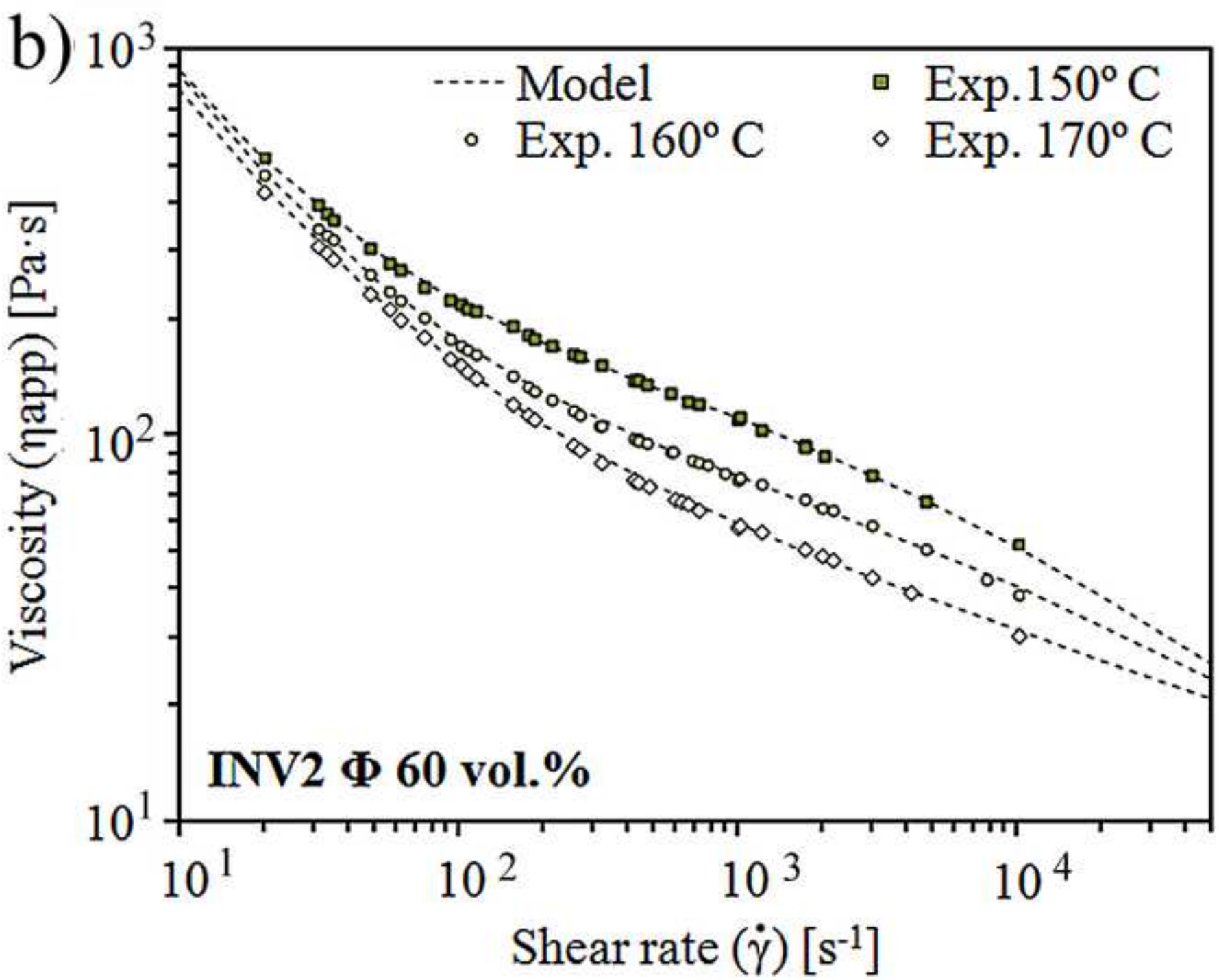

Figure7c

Click here to download high resolution image

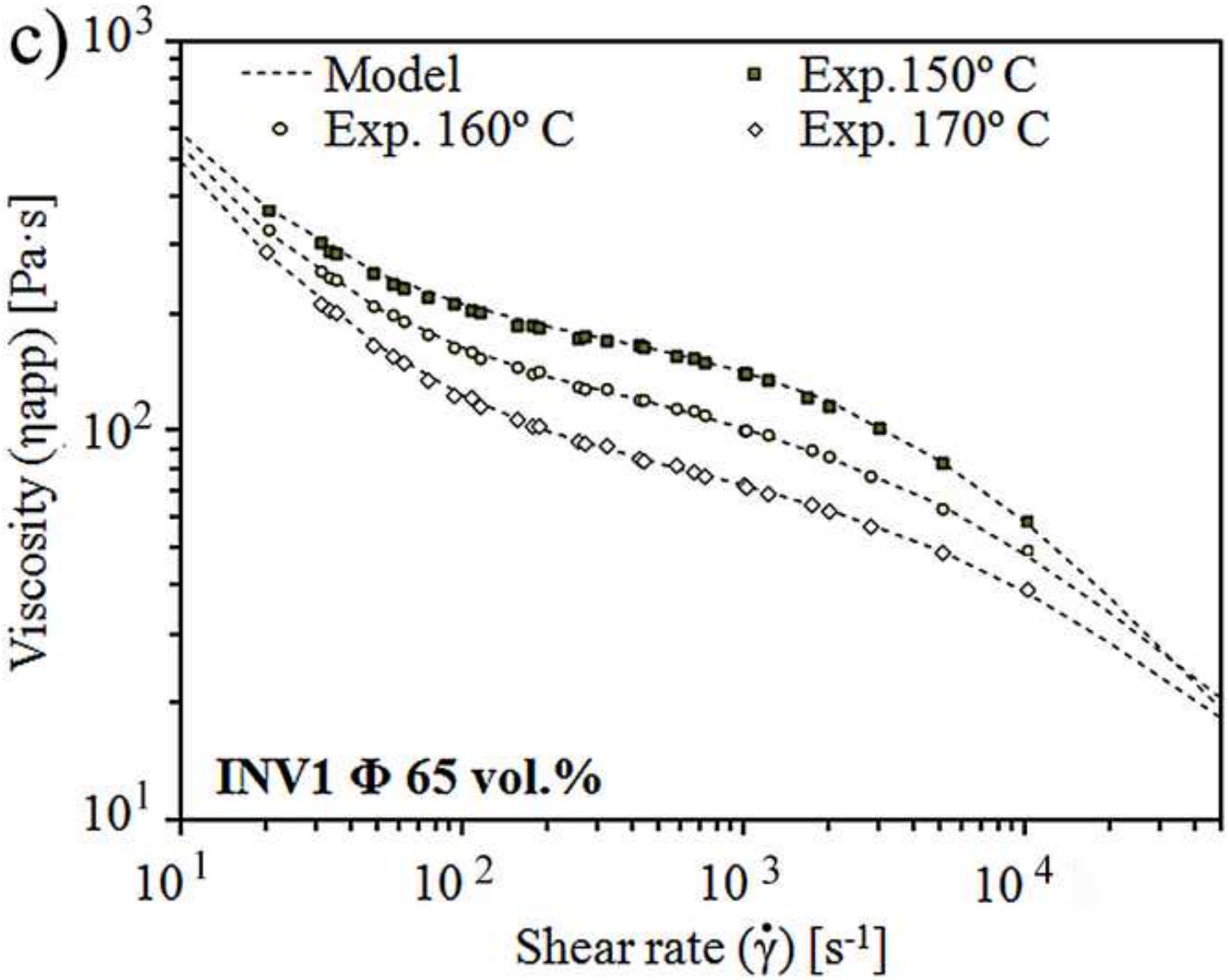

Figure7d

Click here to download high resolution image

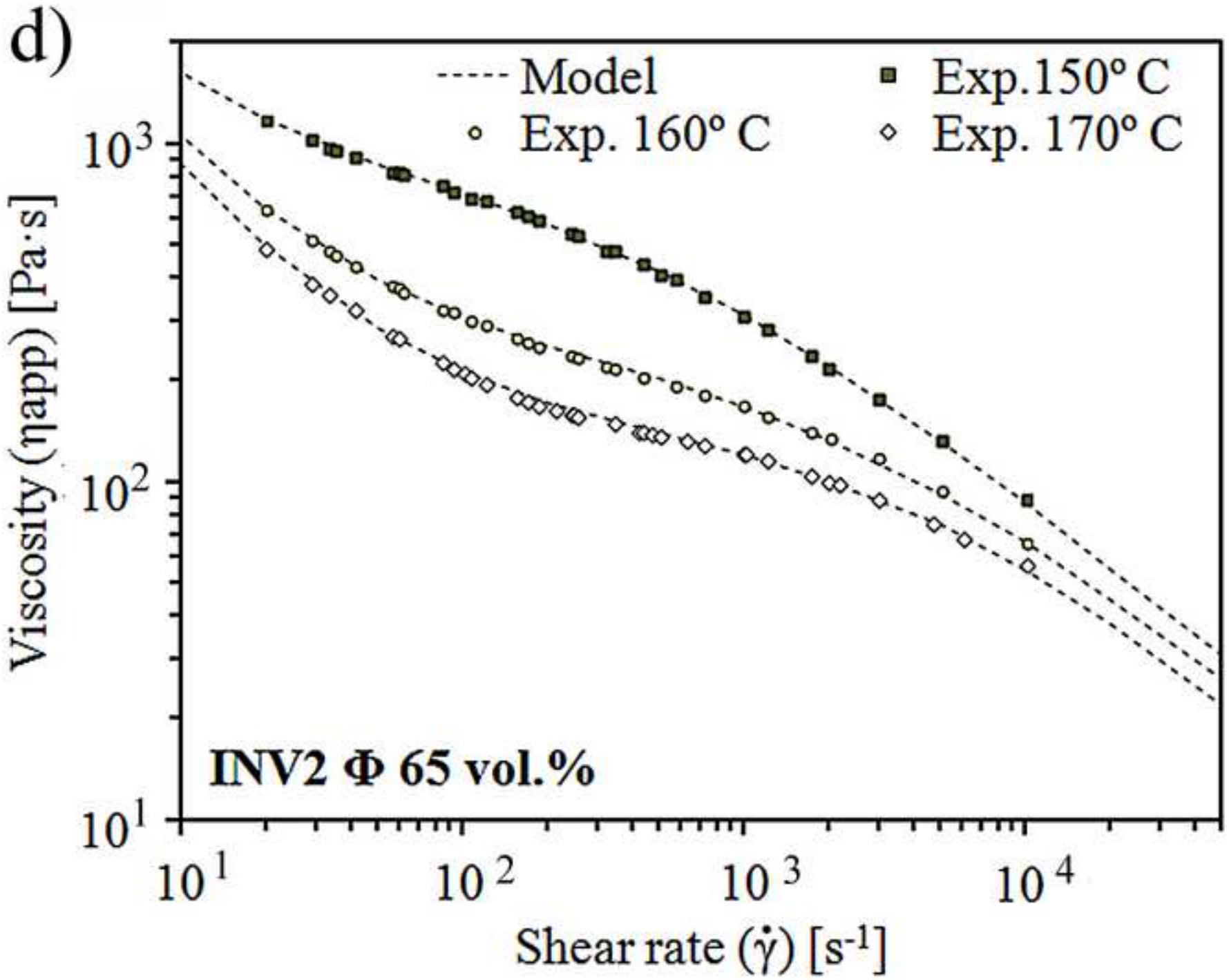

Table1

Table 1 Particle size distribution parameters

	d_{10}	d_{50}	d_{60}	d_{90}	$d_{60}/(d_{10}\cdot d_{50})$	S_w
INV1	5.05	7.69	8.33	11.44	0.214	7.21
INV2	2.60	3.81	4.09	5.29	0.413	8.30

Table2

Table 1 Binder composition

Component	Acetyl*	Butyryl*	Hydroxyl*	%vol
CAB381-0.1	13	37	1.5	30
CAB551-0.01	2	53	1.5	10
PEG 20k	-	-	-	58
PEG 4k	-	-	-	2

** Percentage of side groups in chain*

Table3

Table 1 Resulting coefficients after non-linear regression experimental data adjustment to a Cross modified model of different measuring conditions.

T	η_0	τ_y	k_{II}	1-n	RSS_P	η_0	τ_y	k_{II}	1-n	RSS_P
	INV1 60 vol.%					**INV2 60 vol.%**				
150	92	1324	$2.12 \cdot 10^{-4}$	0.64	1.91	182	7065	$6.09 \cdot 10^{-4}$	0.53	3.97
160	60	1173	$1.21 \cdot 10^{-4}$	0.60	1.45	129	7393	$6.33 \cdot 10^{-4}$	0.44	0.24
170	46	980	$1.49 \cdot 10^{-4}$	0.53	2.92	342	6483	$6.22 \cdot 10^{-1}$	0.27	0.68
	INV1 65 vol.%					**INV2 65 vol.%**				
150	176	4020	$2.28 \cdot 10^{-4}$	0.86	4.15	879	7958	$2.57 \cdot 10^{-3}$	0.69	1.79
160	131	4036	$2.19 \cdot 10^{-4}$	0.71	4.78	252	7996	$4.65 \cdot 10^{-4}$	0.69	2.12
170	87	4033	$1.46 \cdot 10^{-4}$	0.67	4.03	146	7183	$2.00 \cdot 10^{-4}$	0.76	1.27

T → [ºC] ; η_0 → [Pa·s] ; τ_y → [Pa] ; k_{II}, λ → [s] ; a → [] ; n → [ ]

Table4

Table 1 Examples of Mills model coefficients resulting from the fitting of experimental data curves at different temperatures and shear rates

	1000 s^{-1}					10000 s^{-1}				
160 °C	**A**	**m**	**Φ_{crit}**	**R^2**	**RSS_p**	**A**	**m**	**Φ_{crit}**	**R^2**	**RSS_p**
INV1	2.13	0.59	71.2	**0.99**	**6.89**	6.37	4.84	70.6	**1.00**	**1.21**
INV2	0.07	0.019	68.7	**0.99**	**9.90**	6.04	5.14	68.1	**1.00**	**0.91**
170 °C	**A**	**m**	**Φ_{crit}**	**R^2**	**RSS_p**	**A**	**m**	**Φ_{crit}**	**R^2**	**RSS_p**
INV1	0.79	0.28	69.9	**0.99**	**2.33**	0.78	0.31	69.5	**1.00**	**0.77**
INV2	0.015	0.004	68.8	**0.99**	**14.86**	5.22	3.28	68.4	**1.00**	**2.10**

Table5

Table 1 Values of activation energies for INV1 and INV2 at several conditions.

	Φ →	57.5 vol.%		60 vol.%		62.5 vol.%		65 vol.%		67.5 vol.%	
	$\dot{\gamma}$ [s^{-1}]	E [kJ/mol]	R^2	E [kJ/mol]	R^2	E [kJ/mol]	R^2	E [kJ/mol]	R^2	E [kJ/mol]	R^2
INV2	100	49.0	1.00	29.4	0.98	39.3	0.97	94.5	0.97	48.5	0.99
	1000	60.6	1.00	48.7	1.00	48.1	1.00	73.7	0.98	51.8	1.00
	10000	52.9	0.99	38.0	1.00	34.6	0.96	34.9	0.99	91.2	1.00
INV1	100			50.0	1.00	47.5	0.99	41.6	0.99	78.31	1.00
	1000	-		52.5	1.00	52.1	0.99	51.9	1.00	52.6	0.98
	10000			40.6	0.99	35.7	1.00	32.6	1.00	41.26	1.00

Table6

Table 1 Resulting coefficients after curve fitting with the model described in Eq.1 of the experimental points at different temperatures. Φ=65 vol.%, Φ_{crit}=68.6 vol.%, Ea=42.3 kJ/(mol·K).

	C_u/d_{50}	T [K]	η_o [Pa]	n	m	k [s]	τ_y [Pa]	RSSp	R^2
INV2	**0.41**	**423**	105.49	0.59	0.98	$4.37 \cdot 10^3$	1060.0	0.22	1.00
INV1	**0.21**	**423**	45.55	0.77	0.97	$3.22 \cdot 10^4$	1059.8	0.02	1.00
INV2	**0.41**	**433**	31.35	0.56	0.98	$9.78 \cdot 10^4$	1059.5	0.18	1.00
INV1	**0.21**	**433**	32.68	0.56	0.97	$4.95 \cdot 10^4$	1059.4	0.06	1.00
INV2	**0.41**	**443**	20.71	0.59	0.95	$4.28 \cdot 10^4$	1060.0	0.06	1.00
INV1	**0.21**	**443**	21.76	0.50	0.97	$3.96 \cdot 10^4$	1059.9	0.05	1.00

Table7

Table 1 Average values of η_o, m and n at different solid loading values for INV2

Φ [vol.%]	**η_o [Pa]**	**m**	**n**
57.5	63.8	0.60	0.27
60	21.0	1.30	0.31
62.5	26.0	1.10	0.34
65	52.3	0.97	0.58

English languaje corection invoice

Click here to download Supplementary Material: downloadInvoice.cfm